Empirical Valence Bond Simulations of the Hydride Transfer Step in the Monoamine Oxidase B Catalyzed Metabolism of Dopamine

RUNNING TITLE
EVB Simulations of Hydride Transfer in MAO B

Matej Repič,[†] Robert Vianello,[‡] Miha Purg,[†] Fernanda Duarte,[§] Paul Bauer,[§] Shina C. L. Kamerlin,[,§] and Janez Mavri*[,†]*

[†]Laboratory for Biocomputing and Bioinformatics, National Institute of Chemistry, Hajdrihova 19, SI-1000 Ljubljana, Slovenia

[‡]Quantum Organic Chemistry Group, Ruđer Bošković Institute, Bijenička cesta 54, HR-10000 Zagreb, Croatia

[§]Department of Cell and Molecular Biology, Uppsala University, Uppsala Biomedical Centre, Box 596, SE-751 24 Uppsala, Sweden

* Correspondence should be addressed to Janez Mavri (janez.mavri@ki.si) and Shina C. L. Kamerlin (kamerlin@icm.uu.se).

KEYWORDS

computational chemistry, enzyme catalysis, kinetics, neurotransmitters, flavins

ABSTRACT

Monoamine oxidases (MAOs) A and B are flavoenzymes responsible for the metabolism of biogenic amines such as dopamine, serotonin and noradrenaline. In this work, we present atomic details of the rate-limiting step of dopamine degradation by MAO B, which consists of the hydride transfer from the methylene group of the substrate to the flavin moiety of the FAD prosthetic group. This article builds on our previous quantum chemical study of the same reaction using a cluster model (Vianello et al., *Eur. J. Org. Chem.* (**2012**) 7057), but now considering the full dimensionality of the hydrated enzyme with extensive configurational sampling. We show that MAO B is specifically tuned to catalyze the hydride transfer step from the substrate to the flavin moiety of enzyme and that it lowers the activation barrier by 12.3 kcal/mol compared to the same reaction in aqueous solution, a rate enhancement of more than 9 orders of magnitude. Taking into account the deprotonation of the substrate prior to the hydride transfer reaction assuming 1.9 kcal/mol, the activation barrier in the enzyme is calculated to be 16.1 kcal/mol, in excellent agreement with the experimental value of 16.5 kcal/mol. Additionally, we demonstrate that the protonation state of the active site residue Lys296 does not have an influence on the hydride transfer reaction.

INTRODUCTION

Monoamine oxidases (MAO) A and B are flavoenzymes involved in the metabolism of biogenic amines that include the monoamine neurotransmitters dopamine, serotonin and some histamine metabolites.[1,2] MAOs regulate the concentrations of neurotransmitters in the central and peripheral nervous systems, having a major impact on cardiac output, blood pressure, sleep, mood, cognition, and movement.[3,4] The two isoforms, MAO A and MAO B, differ in tissue distribution, substrate selectivity and inhibitor susceptibility.[5-8] Inhibitors that act mainly on MAO A are used in the treatment of depression due to their ability to raise serotonin concentrations, while inhibitors of MAO B decrease dopamine degradation and improve motor control in patients with Parkinson disease.[9] Inhibition of MAOs may also have a significant neuroprotective effect, since the products of its catalytic reaction are hydrogen peroxide, aldehydes, and ammonia, which contribute to oxidative stress in the cell.[10-12]

MAOs convert amines to the corresponding imines by essentially transferring two electrons and two protons from the substrate to the flavin moiety of the covalently bound FAD prosthetic group, transforming the latter to $FADH_2$. The resulting imine non-enzymatically reacts with water, either in the enzyme or in the cytoplasm, and decomposes to the corresponding aldehyde and ammonia (Figure 1).[13]

Despite widespread use of MAO inhibitors and numerous experimental[14-17] and computational[18-21] studies there is still no consensus about the catalytic mechanism on atomic scale. The fundamental catalytic proposals to date are 1) the polar nucleophilic mechanism,[14] 2) the single electron transfer or radical mechanism,[16] and 3) the hydride transfer mechanism[17] (Figure 2).

It has been established by studies on deuterated substrate analogues that the rate-limiting step is the cleavage of a carbon-hydrogen bond vicinal to the amino group[14,22] and hence the catalytic proposals differ in the nature of the hydrogen transfer, namely a proton transfer in 1), a hydrogen atom transfer in 2) and a hydride transfer in 3). While the single electron transfer mechanism has been mainly ruled out by EPR studies,[23] stopped-flow kinetic determinations,[24] lack of magnetic field influence on the reaction,[25] and molecular simulations,[26] the question whether MAOs operate by the polar nucleophilic or hydride transfer mechanism remains open. Miller and Edmondson[14] proposed the polar nucleophilic mechanism on the basis of a structure-activity study on a series of para-substituted benzylamine analogues, which showed that electron-withdrawing groups enhanced the rate of the reaction in human MAO A.[14] An analogous study performed on rat MAO A also showed a similar correlation, in line with the polar nucleophilic mechanism.[27] Contrary to the general assumption that both isoforms utilize the same mechanism a study on human MAO B showed an inverse correlation,[28] suggesting positive charge build-up at the transition state, thus supporting the hydride transfer mechanism. In this study, the authors proposed that the rate-limiting step in human MAO A is proton transfer, whereas in human MAO B it is hydride transfer. However, the same authors had previously ruled out hydride transfer in human MAO B based on the nitrogen secondary kinetic isotope effects.[29]

On the basis of similarities in continuous wave electronic paramagnetic resonance spectrum between D-amino acid oxidase, which was determined to operate by a hydride transfer mechanism,[30] and monoamine oxidase Kay et al. suggested that hydride transfer mechanism should be considered for MAO as well.[31] The availability of high-resolution crystal structures of MAO A[32] and MAO B[33] has opened the possibility to study the catalytic reaction by computational approaches.[18] In recent years, there have been several computational studies

showing the prevailing energetic feasibility of the hydride transfer mechanism.[26,34,35] Our group performed the first quantum mechanical study that convincingly demonstrated the feasibility of hydride transfer mechanism and showed by the NBO analysis that, because of the strong electron donating ability of the vicinal amino group, the atomic charge on the α-carbon atom of the substrate remains negative upon the hydride anion abstraction, which explains why in some instances the reaction could be facilitated even by the electron withdrawing substituents,[26] in line with experimental findings.[14,27] We also proposed the formation of an adduct that follows the hydride transfer and the subsequent deprotonation from the amino group to the N1 atom of flavin, resulting in neutral imine and $FADH_2$ co-factor (Figure 3).[26] Akyüz and Erdem later utilized the ONIOM QM/MM approach to assess the energetics of hydride transfer and also arrived to the conclusion that hydride transfer is the most likely mechanism.[34] Following their previous study, Atalay and Erdem performed a comparative computational study on a series of model systems and again demonstrated the prevailing feasibility of the hydride transfer reaction over the proton transfer reaction,[35] in agreement with our results.[26] Recently, Abad et al. performed a QM/MM study on human MAO B and showed there is substantial charge transfer from the substrate to flavin in the reactants and concluded that these results support the polar nucleophilic mechanism.[20] However, we must emphasize that in our previous study, using a QM cluster model of the MAO B active site, we did not observe any such charge transfer[26] and that Abad et al. failed to obtain the substrate-flavin adduct, which was originally proposed to facilitate the proton transfer[14] (Figure 2).

In this article, we extend our static cluster model study of the rate-limiting step in MAO B to a fluctuating, full enzyme model, evaluating free energies using a semi-empirical QM/MM approach with extensive configurational sampling. Specifically, the quantum subsystem was

described by the empirical valence bond (EVB) method of Warshel and co-workers,[36] allowing for direct evaluation of the catalytic effect of MAO B by comparing the activation free energy in enzyme to the corresponding reference reaction in gas phase or aqueous solution.[37,38] We show that the MAO B enzyme is specifically tuned to catalyze the hydride transfer step from the substrate to the FAD cofactor and that it lowers the activation barrier by 12.3 kcal/mol compared to the aqueous solution, a rate enhancement of more than 9 orders of magnitude. Additionally, we demonstrate that the protonation state of Lys296 does not have an effect on the reductive half-reaction of the enzyme.

COMPUTATIONAL METHODS

Catalysis is the reaction rate enhancement relative to the reference reaction. The ideal reference state for an enzymatic reaction is the corresponding uncatalyzed reaction in aqueous solution, since biology occurs in aqueous solution.[39] However, considering the lack of direct experimental observables in aqueous solution, our calculated reference state for the MAO B catalyzed reaction is the corresponding hydride transfer in vacuum, as this is the state for which one is most likely to obtain reliable estimates of the activation barrier using accurate quantum chemical approaches (see Results and Discussion). For the gas phase reference reaction between lumiflavin and dopamine we used the optimized geometries of the reactants and transition state from our previous study.[26] The gas phase energetics of the reaction were calculated using the M06-2X density functional developed by Truhlar and co-workers[40] in conjunction with the 6-31+G(d,p) basis set, using the Gaussian09 suite of programs.[41] The identity of the transition state structure was confirmed by frequency analysis and intrinsic reaction coordinate (IRC)

calculations.[42-45] All energy values were corrected to include the thermal correction to the Gibbs free energy as described in reference 46.

For the subsequent empirical valence bond (EVB) calculations, we used the MOLARIS simulation package and the ENZYMIX force field,[47] with EVB activation barriers being obtained using the standard free energy perturbation/umbrella sampling (FEP/US) approach outlined in reference [48]. The atomic coordinates were obtained from the high-resolution (1.6 Å) crystal structure of MAO B in complex with 2-(2-benzofuranyl)-2-imidazoline),[49] obtained from the Protein Data Bank[50] (accession code 2XFN). The protein structure was prepared for EVB simulation in UCSF Chimera[51] by removing water and hetero ligands (2-(2-benzofuranyl)-2-imidazoline and N-dodecyl-N,N-dimethyl-3-ammonio-1-propanesulfonate) and keeping only the side chains with the highest occupancy where multiple conformations were present in the crystal structure. The charges of all relevant structures were fitted to the electrostatic potential according to the CHelpG scheme with UFF radii and calculated at the (CPCM)/B3LYP/6-31+G(d,p) level,[52-54] utilizing the conductor-like polarized continuum (CPCM) solvent reaction field model of Tomasi and co-workers,[55] as implemented in Gaussian09 suite of programs. The dopamine substrate was manually placed into the MAO B active site, based on optimizing the interactions of the dopamine with its environment using chemical intuition. As there is room for substantial conformational variability within the binding pocket, multiple conformations of the dopamine were tested.

EVB calculations were performed *in vacuo* (the reference state calibrated to QM calculations), as well as in an all-atom representation of aqueous solution and in the MAO B active site, to examine the effect of changing the environment on the reaction barrier. For all EVB calculations we used the same EVB region, consisting of lumiflavin moiety and dopamine (FAD and

dopamine in the enzyme). The reactive system, except for gas phase calculations, was solvated according to the surface-constrained all atom solvent model (SCAAS),[56] using a spherical cut-off of 20 Å measured from the centroid of the reacting atoms. The spherical droplet was embedded in a 3 Å cubic grid of Langevin dipoles (22 Å spherical cut-off), which was in turn placed in a continuum with the dielectric constant of water. The cut-off for long-range interactions was 10 Å and the neighbor list was updated every 30 steps. All systems were subsequently relaxed with a step size of 1 fs for 50 ps at 30 K, 100 ps at 100 K and 500ps at 300 K using the ENZYMIX force field as implemented in the MOLARIS simulation package.[56] The relaxed system was mutated from a reactant diabatic state to a product diabatic state (Figure 4) in 51 mapping frames, each consisting of a molecular dynamics simulation of 30 ps, using a 1 fs time step, for a total simulation time of 1530 ps. The EVB simulation of the reactive trajectory was performed 10 times starting from different initial configurations, giving rise to ten independent free energy profiles.

RESULTS AND DISCUSSION

EVB parameterization and calculation of the energetics of the gas-phase reference reaction

Evaluation of the catalytic effect of an enzyme requires a definition of the reference state. The ideal reference state for an enzymatic reaction is the corresponding uncatalyzed reaction in aqueous solution. The same mechanism is assumed to be operational in the gas phase, aqueous solution and in protein. To our best knowledge, there are no reports in the literature about the kinetics of uncatalyzed reactions between flavins and phenethylamines or suitable model compounds. Thus, an accurate value of the activation barrier in aqueous solution cannot be obtained, although there were several studies performed on other hydride transfer reactions

between various substrates and NAD^+ cofactor, using model systems.[57-59] The work performed by Hamilton[60] and later by Mariano[61] has shown that flavins react with amines and alcohols in aqueous solution on a timescale of days, but no time-resolved reaction profile is available.

Considering the lack of solution-phase experimental data, we parameterized our EVB Hamiltonian to reproduce reliable M062X/6-31+G(d,p) energetics *in vacuo* ($\Delta G^{\ddagger}_{gas}$ and ΔG°_{gas}). The system was subsequently moved to aqueous solution and to the MAO B active site using the same parameter set. This is a valid approximation, due to the demonstrated phase-independence of the EVB off-diagonal (H_{ij}) coupling term.[62] This approach allows us to 1) explore the effect of changing the environment both to aqueous solution and to the more complex environment of the MAO B active site, and also 2) to obtain an approximation of the catalytic enhancement relative to aqueous solution using the EVB calculations. The gas phase reference reaction is an established approach.[63,64]

We have shown in our previous study using the cluster model that transfer of the hydride anion from dopamine to flavin is the rate-limiting step.[26] To model the hydride transfer step by EVB, we need to know the activation free energy ($\Delta G^{\ddagger}_{gas}$) and the free energy ($\Delta G^{\circ}_{gas}$) of the reference reaction. While it is possible to obtain $\Delta G^{\ddagger}_{gas}$, the calculation of ΔG°_{gas} is complicated by the fact that, in the gas phase, the resulting $FADH^-$ anion and dopamine cation form an adduct immediately upon hydride transfer (Figure 5). The absence of a stable transient intermediate, which represents the EVB product of the hydride transfer step, can be explained by the high energetic penalty associated with separating the charges in the gas phase, as is also reflected in the very high endergonicity of the reaction of 24.9 kcal/mol. To approximate the relative energy of the transient intermediate we therefore selected the point in the IRC profile where the structure of $FADH^-$ moiety matches the geometry of the gas-phase optimized $FADH^-$.

Furthermore, the IRC profile shows a marked change in the potential energy surface around the same point, indicating a viable transient intermediate. We must emphasize, that calibrating the EVB reaction to reproduce the reaction free energy 5 kcal/mol higher or lower than the energy of the transient intermediate does not appreciably influence the catalytic effect of the enzyme. This indicates that an estimate, rather than a precise value, of free energy of the reaction in the gas phase, is sufficient to calculate the catalytic effect of the enzyme.

Full geometrical optimization of the reactant, the transition state, and the adduct, including the thermal correction to Gibbs free energy, shows that the transition state and the adduct are 32.8 kcal/mol and 10.0 kcal/mol higher in energy than the reactants, respectively. As stated before, the transient intermediate cannot be fully optimized due to the formation of the adduct during the optimization. Nevertheless, taking into account the thermal correction, the product is 24.9 kcal/mol higher in energy than the reactants. The EVB gas-phase shift and coupling parameter were thus parameterized to reproduce the $\Delta G^{\ddagger}_{gas}$ of 32.8 kcal/mol and the ΔG°_{gas} of 24.9 kcal/mol.

The effect of the aqueous solution and the enzyme environment

Using the same parameters as in the gas-phase EVB simulation the calculations are repeated in the aqueous solution and in the protein to assess the effect of the environment on the energetics of the hydride transfer reaction. The results are summarized in Table II and Figure 6.

Studies of the hydride transfer on a series of NAD^+ analogues in aqueous solution have shown that the typical free energy barrier for hydride transfer is ~20 kcal/mol.[65,66] However, while FAD and NAD^+ analogues are both very good acceptors of the hydride ion, NADH is a significantly better hydride donor than the α-CH_2 group of dopamine. On this basis, we assume that the barrier for the hydride transfer between dopamine and FAD must be considerably higher. Our

calculations in the aqueous solution confirm this assumption as the reaction has a barrier of 26.5 kcal/mol, while the free energy of the reaction is drastically lowered to 4.2 kcal/mol. The decrease in the activation barrier and an even more pronounced decrease in the free energy demonstrate the favorable effect of solvation on the hydride transfer reaction. Lending more credence to the proposed mechanism, the angle between the hydride donor atom, the hydride, and the hydride acceptor atom (C-H-N5 angle in Figure 7) in the transition state is 157.3 degrees, in perfect agreement with the theoretical study on hydride transfer between FAD and NADH analogues performed by Andrés et al.[67] that obtained values ranging from 158 to 161 degrees employing various levels of theory.

Taking the reaction into the MAO protein environment, we see further reduction of the barrier to 14.2 kcal/mol, while the reaction becomes exergonic with the reaction free energy of -0.6 kcal/mol. The reduction in the activation barrier compared to the aqueous solution is 12.3 kcal/mol, which corresponds to a rate-enhancement of more than 9 orders of magnitude. The reaction is not overly exergonic, thereby avoiding product entrapment, which could occur in the case of excess reaction free energy.

Experimental studies have shown that the deprotonated form of the substrate is essential for the reaction, but that the substrate is likely bound to the active site in its protonated form.[68] Therefore, an intraenzymatic deprotonation must take place, which can be accomplished by several water molecules present in the enzyme. We have calculated in a previous study, that the deprotonation of the enzyme-bound dopamine to the bulk solvent costs 1.9 kcal/mol in terms of free energy,[69] which, added to the calculated barrier for the reaction of 14.2 kcal/mol, gives an activation free energy of 16.1 kcal/mol. The latter value is in excellent agreement with the

experimental value of 16.5 kcal/mol,[15] strongly supporting the proposed hydride transfer mechanism.

We have also observed that, for the efficient catalysis, the amino group of the substrate must orient toward the O4 atom of FAD to allow for hydrogen bonding (Figure 7). There is also considerably more space on this side of the active site cavity compared to the other, which allows for better accommodation of the substrate and proper positioning for the hydride transfer. Studies have shown, that MAO preferentially cleaves the pro-R hydrogen atom (H atom in Figure 7)[14,70] and in this configuration the pro-R hydrogen atom of the dopamine CH_2 group is perfectly aligned to enable the hydride transfer (Figure 7).

The effect of Lys296 protonation state on the hydride transfer reaction

The Lys296 residue is a part of the FAD-H_2O-Lys296 motif conserved in many flavin-dependent oxidases[71] and might play a significant role in the MAO catalysis. Although there is substantial agreement in the flavooxidase community that the role of the lysine is to activate the oxygen and facilitate the regeneration of the enzyme and that it does not have a role in the oxidation of the substrate,[11,12] we have performed our calculations with both the ionized and unionized form of Lys296 to assess the effect of the ionization state of this residue on the hydride transfer reaction.

We have shown in a very recent study, that the pK_a of the Lys296 residue with dopamine docked in the active site 10.8[72] and is, thus, predominantly present in its charged form at the physiological pH, however, the preferred ionization state is not necessarily the catalytically active one. Our results show, that the protonation state of Lys296 does not affect the reductive half-reaction of MAO B and that the barrier for the reaction is virtually unchanged at 14.0

kcal/mol (Table II). This finding is in full agreement with the results of Henderson-Pozzi and Fitzpatrick, which showed that in mouse polyamine oxidase the protonation state of the corresponding lysine only affects the oxidative half-reaction.[71]

CONCLUSION

By using the empirical valence bond QM/MM approach we showed that MAO B lowers the barrier of the hydride transfer reaction by 12.3 kcal/mol, what corresponds to a rate-enhancement of more than 9 orders of magnitude compared to the corresponding reaction in aqueous solution. The barrier for the enzymatic reaction starting from the deprotonated substrate is 14.2 kcal/mol. Taking into account the free energy cost of dopamine deprotonation in the active site prior to the enzymatic reaction the reaction barrier is 16.1 kcal/mol, in excellent agreement with the available experimental value of 16.5 kcal/mol.[15] Moreover, we have also shown that the protonation state of Lys296 does not have an effect on the hydride transfer reaction in MAO B, which is consistent with the proposed function of the lysine as stabilizing the superoxide required for the regeneration of the enzyme. In conjunction with additional experimental and computational work, the data presented here improve the understanding of mechanism of the catalytic activity and irreversible inhibition of MAO B, which can allow for the design of novel and improved MAO B inhibitors for antiparkinsonian and neuroprotective use.

ACKNOWLEDGMENT

M.R. and J.M. would like to thank the Slovenian Research Agency for financial support in the framework of the program group P1–0012 and within the corresponding research project contract

No. J1–2014. R. V. gratefully acknowledges the European Commission for an individual FP7 Marie Curie Career Integration Grant (contract number PCIG12–GA–2012–334493). Part of this work was also supported by COST Action CM1103. S.C.L.K. would like to thank the Swedish research council (VR, grant 2010-5026) for funding this work.

SUPPORTING INFORMATION

Supporting information includes naming and numbering of the EVB (reacting) atoms in the different EVB states and the parameters used in the EVB calculations.

REFERENCES

1. Nestler EJ, Hyman SE, Malenka RC. Catecholamines. In: Nestler EJ, Hyman SE, Malenka RC, editors. Molecular Neuropharmacology: A Foundation for Clinical Neurosciece. New York: McGraw Hill; 2001. p 167-190.

2. Harsing LG. Dopamine and the Dopaminergic Systems of the Brain. In: Vizi ES, editor. Handbook of Neurochemisty and Molecular Neurobiology: Neurotransmitter Systems. New York: Springer; 2008. p 151-170.

3. Goodman LS, Gilman A, Brunton LL. Neurotransmission and the Central Nervous System. Goodman & Gilman's Pharmacological Basis of Therapeutics. New York: McGraw-Hill Medical; 2008. p 293-320.

4. Strolin Benedetti M, Tipton KF. Monoamine Oxidases and Related Amine Oxidases as Phase I Enzymes in The Metabolism of Xenobiotics. J Neural Transm, Suppl 1998;52:149-171.

5. Johnston JP. Some Observations Upon a New Inhibitor of Monoamine Oxidase in Brain Tissue. Biochem Pharmacol 1968;17(7):1285-1297.

6. Knoll J, Magyar K. Some Puzzling Pharmacological Effects of Monoamine Oxidase Inhibitors. Adv Biochem Psychopharmacol 1972;5:393-408.

7. Westlund KN. The Distribution of Monoamine Oxidases A and B in Normal Human Brain. In: Lieberman AN, editor. Monoamine oxidase inhibitors in neurological diseases: CRC Press, 1994; 1994. p 1-20.

8. Thorpe LW, Westlund KN, Kochersperger LM, Abell CW, Denney RM. Immunocytochemical Localization of Monoamine Oxidases A And B in Human Peripheral Tissues and Brain. J Histochem Cytochem 1987;35(1):23-32.

9. Youdim MBH, Edmondson D, Tipton KF. The Therapeutic Potential of Monoamine Oxidase Inhibitors. Nat Rev Neurosci 2006;7(4):295-309.

10. Edmondson DE. Hydrogen Peroxide Produced by Mitochondrial Monoamine Oxidase Catalysis: Biological Implications. Curr Pharm Des 2014;20(2):155-160.

11. Gadda G. Oxygen Activation in Flavoprotein Oxidases: The Importance of Being Positive. Biochemistry 2012;51(13):2662-2669.

12. Klinman JP. How Do Enzymes Activate Oxygen Without Inactivating Themselves? Acc Chem Res 2007;40(5):325-333.

13. Husain M, Edmondson DE, Singer TP. Kinetic-Studies on the Catalytic Mechanism of Liver Monoamine-Oxidase. Biochemistry 1982;21(3):595-600.

14. Miller JR, Edmondson DE. Structure-Activity Relationships in the Oxidation of Para-Substituted Benzylamine Analogues by Recombinant Human Liver Monoamine Oxidase A. Biochemistry 1999;38(41):13670-13683.

15. Edmondson DE, Binda C, Wang J, Upadhyay AK, Mattevi A. Molecular and Mechanistic Properties of the Membrane-Bound Mitochondrial Monoamine Oxidases. Biochemistry 2009;48(20):4220-4230.

16. Silverman RB. Radical Ideas About Monoamine-Oxidase. Acc Chem Res 1995;28(8):335-342.

17. Gaweska H, Fitzpatrick PF. Structures and Mechanism of the Monoamine Oxidase Family. Biomol Concepts 2011;2(5):365-377.

18. Erdem SS, Karahan O, Yildiz I, Yelekçi K. A Computational Study on the Amine-Oxidation Mechanism of Monoamine Oxidase: Insight Into the Polar Nucleophilic Mechanism. Org Biomol Chem 2006;4(4):646-658.

19. Erdem SS, Büyükmenekşe B. Computational Investigation on the Structure-Activity Relationship of the Biradical Mechanism for Monoamine Oxidase. J Neural Transm 2011;118(7):1021-1029.

20. Abad E, Zenn RK, Kästner J. Reaction Mechanism of Monoamine Oxidase from QM/MM Calculations. J Phys Chem B 2013;117(46):14238-14246.

21. Akyüz MA, Erdem SS, Edmondson DE. The Aromatic Cage in the Active Site of Monoamine Oxidase B: Effect on the Structural and Electronic Properties of Bound Benzylamine and P-Nitrobenzylamine. J Neural Transm 2007;114(6):693-698.

22. Klinman JP, Matthews RG. Calculation of Substrate Dissociation-Constants from Steady-State Isotope Effects in Enzyme-Catalyzed Reactions. J Am Chem Soc 1985;107(4):1058-1060.

23. Tan A, Glantz MD, Piette LH, Yasunobu KT. Electron-Spin-Resonance Analysis of the FAD in Bovine Liver Monoamine-Oxidase. Biochem Biophys Res Commun 1983;117(2):517-523.

24. Nandigama RK, Edmondson DE. Structure-Activity Relations in the Oxidation of Phenethylamine Analogues by Recombinant Human Liver Monoamine Oxidase A. Biochemistry 2000;39(49):15258-15265.

25. Miller JR, Edmondson DE, Grissom CB. Mechanistic Probes of Monoamine-Oxidase-B Catalysis - Rapid-Scan Stopped-Flow and Magnetic-Field Independence of the Reductive Half-Reaction. J Am Chem Soc 1995;117(29):7830-7831.

26. Vianello R, Repič M, Mavri J. How are Biogenic Amines Metabolized by Monoamine Oxidases? Eur J Org Chem 2012;2012(36):7057-7065.

27. Wang J, Edmondson DE. (2)H Kinetic Isotope Effects and pH Dependence of Catalysis as Mechanistic Probes of Rat Monoamine Oxidase A: Comparisons with the Human Enzyme. Biochemistry 2011;50(35):7710-7717.

28. Orru R, Aldeco M, Edmondson DE. Do MAO A and MAO B Utilize the Same Mechanism for the C-H Bond Cleavage Step in Catalysis? Evidence Suggesting Differing Mechanisms. J Neural Transm 2013;120(6):847-851.

29. Macmillar S, Edmondson DE, Matsson O. Nitrogen Kinetic Isotope Effects for the Monoamine Oxidase B-Catalyzed Oxidation of Benzylamine and (1,1-(2)H(2))Benzylamine: Nitrogen Rehybridization and CH Bond Cleavage Are Not Concerted. J Am Chem Soc 2011;133(32):12319-12321.

30. Umhau S, Pollegioni L, Molla G, Diederichs K, Welte W, Pilone MS, Ghisla S. The x-ray structure of D-amino acid oxidase at very high resolution identifies the chemical mechanism of flavin-dependent substrate dehydrogenation. 2000;97(23):12463-12468.

31. Kay CW, El Mkami H, Molla G, Pollegioni L, Ramsay RR. Characterization of the covalently bound anionic flavin radical in monoamine oxidase a by electron paramagnetic resonance. J Am Chem Soc 2007;129(51):16091-16097.

32. De Colibus L, Li M, Binda C, Lustig A, Edmondson DE, Mattevi A. Three-Dimensional Structure of Human Monoamine Oxidase A (MAO A): Relation to the Structures of Rat MAO A and Human MAO B. Proc Natl Acad Sci U S A 2005;102(36):12684-12689.

33. Binda C, Hubalek F, Li M, Edmondson DE, Mattevi A. Crystal Structure of Human Monoamine Oxidase B, A Drug Target Enzyme Monotopically Inserted Into the Mitochondrial Outer Membrane. FEBS Lett 2004;564(3):225-228.

34. Akyüz MA, Erdem SS. Computational Modeling of The Direct Hydride Transfer Mechanism For The MAO Catalyzed Oxidation of Phenethylamine and Benzylamine: ONIOM (QM/MM) Calculations. J Neural Transm 2013;120(6):937-945.

35. Atalay VE, Erdem SS. A Comparative Computational Investigation on the Proton and Hydride Transfer Mechanisms of Monoamine Oxidase Using Model Molecules. Comput Biol Chem 2013;47:181-191.

36. Warshel A, Levitt M. Theoretical Studies of Enzymic Reactions: Dielectric, Electrostatic and Steric Stabilization of the Carbonium Ion in the Reaction of Lysozyme. J Mol Biol 1976;103(2):227-249.

37. Warshel A, Weiss RM. Empirical Valence Bond Calculations of Enzyme Catalysis. Ann N Y Acad Sci 1981;367:370-382.

38. Warshel A, Hwang JK, Åqvist J. Computer Simulations of Enzymatic Reactions: Examination of Linear Free-Energy Relationships and Quantum-Mechanical Corrections in the Initial Proton-Transfer Step of Carbonic Anhydrase. Faraday Discuss 1992(93):225-238.

39. Warshel A, Sharma PK, Kato M, Xiang Y, Liu H, Olsson MH. Electrostatic Basis for Enzyme Catalysis. Chem Rev 2006;106(8):3210-3235.

40. Zhao Y, Truhlar DG. The M06 Suite of Density Functionals for Main Group Thermochemistry, Thermochemical Kinetics, Noncovalent Interactions, Excited States, and Transition Elements: Two New Functionals and Systematic Testing of Four M06-Class Functionals and 12 Other Functionals. Theor Chem Acc 2008;120(1-3):215-241.

41. Frisch MJ, Trucks GW, Schlegel HB, Scuseria GE, Robb MA, Cheeseman JR, Scalmani G, Barone V, Mennucci B, Petersson GA, Nakatsuji H, Caricato M, Li X, Hratchian HP, Izmaylov AF, Bloino J, Zheng G, Sonnenberg JL, Hada M, Ehara M, Toyota K, Fukuda R, Hasegawa J, Ishida M, Nakajima T, Honda Y, Kitao O, Nakai H, Vreven T, Jr. JAM, Peralta JE, Ogliaro F, Bearpark M, Heyd JJ, Brothers E, Kudin KN, Staroverov VN, Kobayashi R, Normand J, Raghavachari K, Rendell A, Burant JC, Iyengar SS, Tomasi J, Cossi M, Rega N, Millam JM, Klene M, Knox JE, Cross JB, Bakken V, Adamo C, Jaramillo J, Gomperts R, Stratmann RE, Yazyev O, Austin AJ, Cammi R, Pomelli C, Ochterski JW, Martin RL, Morokuma K, Zakrzewski VG, Voth GA, Salvador P, Dannenberg JJ, Dapprich S, Daniels

AD, Farkas O, Foresman JB, Ortiz JV, Cioslowski J. Gaussian 09, Revision A.02: Gaussian Inc. Wallingford CT, 2009; 2009.

42. Hratchian HP, Schlegel HB. In: Dykstra CE, Frenking G, S. KK, G. S, editors. Theory and Applications of Computational Chemistry: The First 40 Years. Amsterdam: Elsevier; 2005. p 195-249.

43. Hratchian HP, Schlegel HB. Accurate Reaction Paths Using a Hessian Based Predictor-Corrector Integrator. J Chem Phys 2004;120(21):9918-9924.

44. Hratchian HP, Schlegel HB. Using Hessian Updating to Increase the Efficiency of a Hessian Based Predictor-Corrector Reaction Path Following Method. J Chem Theory Comput 2005;1(1):61-69.

45. Fukui K. The Path of Chemical Reactions - The IRC Approach. Acc Chem Res 1981;14(12):363-368.

46. Ochterski JW. Thermochemistry in Gaussian. 2000.

47. Lee FS, Chu ZT, Warshel A. Microscopic and Semimicroscopic Calculations of Electrostatic Energies in Proteins by the POLARIS and ENZYMIX Programs. J Comp Chem 1993;14(2):161-185.

48. Kamerlin SCL, Warshel A. The Empirical Valence Bond Model: Theory and Applications. Wiley Interdiscip Rev: Comput Mol Sci 2011;1(1):30-45.

49. Bonivento D, Milczek EM, McDonald GR, Binda C, Holt A, Edmondson DE, Mattevi A. Potentiation of Ligand Binding Through Cooperative Effects in Monoamine Oxidase B. J Biol Chem 2010;285(47):36849-36856.

50. Bernstein FC, Koetzle TF, Williams GJB, Meyer EF, Brice MD, Rodgers JR, Kennard O, Shimanouchi T, Tasumi M. Protein Data Bank - Computer-Based Archival File for Macromolecular Structures. J Mol Biol 1977;112(3):535-542.

51. Pettersen EF, Goddard TD, Huang CC, Couch GS, Greenblatt DM, Meng EC, Ferrin TE. UCSF Chimera--A Visualization System for Exploratory Research and Analysis. J Comp Chem 2004;25(13):1605-1612.

52. Becke AD. Density-Functional Thermochemistry .1. The Effect of the Exchange-Only Gradient Correction. J Chem Phys 1992;96(3):2155-2160.

53. Becke AD. Density-Functional Thermochemistry .2. The Effect of the Perdew-Wang Generalized-Gradient Correlation Correction. J Chem Phys 1992;97(12):9173-9177.

54. Becke AD. Density-Functional Thermochemistry .3. The Role of Exact Exchange. J Chem Phys 1993;98(7):5648-5652.

55. Tomasi J, Persico M. Molecular-Interactions in Solution - an Overview of Methods Based on Continuous Distributions of the Solvent. Chem Rev 1994;94(7):2027-2094.

56. Warshel A, King G. Polarization Constraints in Molecular Dynamics Simulation of Aqueous Solutions: The Surface Constraint All Atom Solvent (SCAAS) Model. Chem Phys Lett 1985;121(1–2):124-129.

57. Lu Y, Qu F, Moore B, Endicott D, Kuester W. Hydride Reduction of NAD+ Analogues by Isopropyl Alcohol: Kinetics, Deuterium Isotope Effects and Mechanism. J Org Chem 2008;73(13):4763-4770.

58. Liu Q, Zhao Y, Hammann B, Eilers J, Lu Y, Kohen A. A Model Reaction Assesses Contribution of H-tunneling and Coupled Motions to Enzyme Catalysis. J Org Chem 2012;77(16):6825-6833.

59. Lu Y, Endicott D, Kuester W. Effective Thermal Oxidation of Isopropanol by an NAD+ Model. Tetrahedron Lett 2007;48(36):6356-6359.

60. Brown LE, Hamilton GA. Some Model Reactions and a General Mechanism for Flavoenzyme-Catalyzed Dehydrogenations. J Am Chem Soc 1970;92(24):7225-7227.

61. Kim JM, Bogdan MA, Mariano PS. Mechanistic Analysis of the 3-Methyllumiflavin-Promoted Oxidative Deamination of Benzylamine. A Potential Model for Monoamine Oxidase Catalysis. J Am Chem Soc 1993;115(23):10591-10595.

62. Hong G, Rosta E, Warshel A. Using the Constrained DFT Approach in Generating Diabatic Surfaces and off Diagonal Empirical Valence Bond Terms for Modeling Reactions in Condensed Phases. J Phys Chem B 2006;110(39):19570-19574.

63. Mo Y, Gao J. Ab initio QM/MM simulations with a molecular orbital-valence bond (MOVB) method: application to an SN2 reaction in water. J Comp Chem 2000;21(16):1458-1469.

64. Chandrasekhar J, Smith SF, Jorgensen WL. Theoretical examination of the SN2 reaction involving chloride ion and methyl chloride in the gas phase and aqueous solution. J Am Chem Soc 1985;107(1):154-163.

65. Kong YS, Warshel A. Linear Free-Energy Relationships with Quantum-Mechanical Corrections - Classical and Quantum-Mechanical Rate Constants for Hydride Transfer between Nad(+) Analogs in Solutions. J Am Chem Soc 1995;117(23):6234-6242.

66. Kreevoy MM, Ostovic D, Lee ISH, Binder DA, King GW. Structure Sensitivity of the Marcus-Lambda for Hydride Transfer between NAD+ Analogs. J Am Chem Soc 1988;110(2):524-530.

67. Andres J, Moliner V, Safont VS, Domingo LR, Picher MT. On Transition Structures for Hydride Transfer Step in Enzyme Catalysis. A Comparative Study on Models of Glutathione Reductase Derived from Semiempirical, HF, and DFT Methods. J Org Chem 1996;61(22):7777-7783.

68. Jones TZ, Balsa D, Unzeta M, Ramsay RR. Variations in Activity and Inhibition with pH: The Protonated Amine is the Substrate for Monoamine Oxidase, but Uncharged Inhibitors Bind Better. J Neural Transm 2007;114(6):707-712.

69. Borštnar R, Repič M, Kamerlin SCL, Vianello R, Mavri J. Computational Study of the pKa Values of Potential Catalytic Residues in the Active Site of Monoamine Oxidase B. J Chem Theory Comput 2012;8(10):3864-3870.

70. Li M, Binda C, Mattevi A, Edmondson DE. Functional Role of the Aromatic Cage in Human Monoamine Oxidase B: Structures and Catalytic Properties of Tyr435 Mutant Proteins. Biochemistry 2006;45(15):4775-4784.

71. Henderson Pozzi M, Fitzpatrick PF. A Lysine Conserved in the Monoamine Oxidase Family is Involved in Oxidation of the Reduced Flavin in Mouse Polyamine Oxidase. Arch Biochem Biophys 2010;498(2):83-88.

72. Repič M, Purg M, Vianello R, Mavri J. Examining Electrostatic Preorganization in Monoamine Oxidases A and B by Structural Comparison and pKa Calculations. J Phys Chem B 2014;118(16):4326-4332.

FIGURE LEGENDS

Figure 1. The catalytic cycle of monoamine oxidases is divided into the reductive half-reaction, in which the substrate is metabolized, and oxidative half-reaction, in which the enzyme is regenerated by molecular oxygen. The grey area represents the enzyme interior while the red dot represents the rate-limiting step of the reductive half-reaction.

Figure 2. Three major catalytic proposals for the mechanism of monoamine oxidase. The pivotal point is the nature of the hydrogen transfer, namely a hydrogen atom transfer in the radical mechanism 1), a proton transfer in polar nucleophilic mechanism 2), and a hydride transfer in the direct hydride transfer mechanism 3).

Figure 3. The complete two-step hydride transfer mechanism. In the first step, the hydride is transferred from the substrate to flavin and subsequently a weak covalent adduct is formed. In the following step two water molecules assist a proton transfer from the substrate amino group to the N1 atom of flavin

Figure 4. Diabatic reactant and product states for the rate-limiting step of the two-step hydride transfer mechanism. The product later forms an adduct as shown in Figure 3.

Figure 5. Intrinsic reaction coordinate profile for the reaction between dopamine and flavin model in the gas-phase. The structures corresponding to the red points were subsequently

optimized and thermal correction to Gibbs free energy was included, slightly changing the relative energies (See gas results in Table II.). Note that the transient intermediate in this figure corresponds to EVB product in the main text.

Figure 6. Empirical valence bond free energy profiles for the reaction in the gas-phase (grey), aqueous solution (blue), protein with unionized Lys296 (green), and protein with ionized Lys296 (violet). Note that due to similarity of the energetics for these last two scenarios the profiles almost completely overlap. ε is the generalized reaction coordinate defined by the difference between the potential surfaces of the reactant and product state.

Figure 7. MAO B active site, showing the residues enclosing the active site. The active site residues are shown in gray, FAD prosthetic group in orange, dopamine in light blue, and Lys296 in violet. Note the direction the amino group is pointing to, which facilitates the positioning of the pro-R hydrogen atom for hydride transfer.

TABLES

Table I. Gas-phase optimized energetics of the hydride transfer reaction between dopamine and flavin model at the M06-2X/6-31+G(d,p) level. All values include the thermal correction to Gibbs free energy. Please note that the reactant correspond to the Michaelis complex.

	Reactant	Transition state	Transient intermediate	Adduct
ΔG_{gas}	0.0	32.8	24.9[a]	10.0

[a] Unoptimized geometry (For details see Results and Discussion.)

Table II. Empirical valence bond free energies relative to the reactant. The average over 10 runs is shown with the corresponding standard deviation in the parentheses for the activation free energy ($\Delta G^{\ddagger}$) and reaction free energy ($\Delta G°$), respectively.

	Reactant	Transition state ($\Delta G^{\ddagger}$)	Products ($\Delta G°$)[c]
Gas	0.0	32.8 (0.9)	24.9 (1.6)
Water	0.0	26.5 (1.3)	4.2 (1.1)
Protein[a]	0.0	14.2 (0.5)	-0.6 (1.2)
Protein[b]	0.0	14.0 (0.8)	-1.6 (0.9)

[a] Lys296 unionized during the simulation.

[b] Lys296 ionized during the simulation.

[c] Note that the product corresponds to the geometry of the transient intermediate.

FIGURES

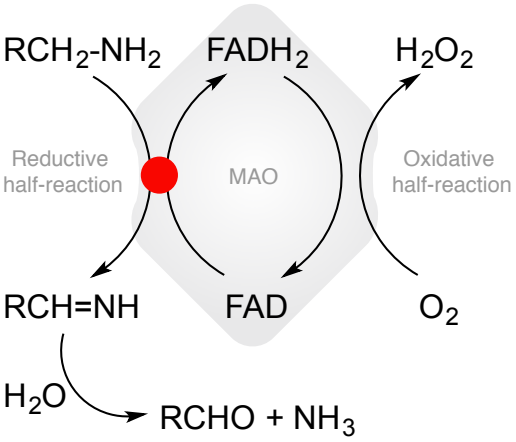

Figure 1.

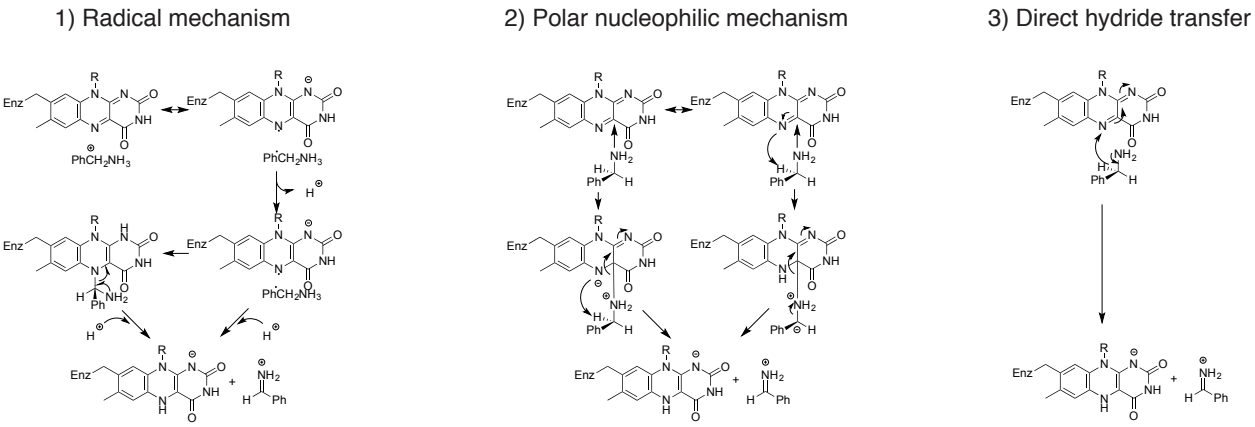

Figure 2.

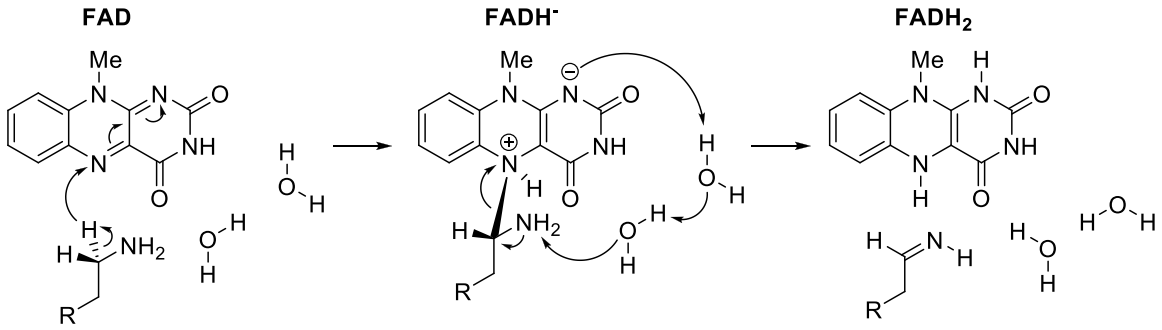

Figure 3.

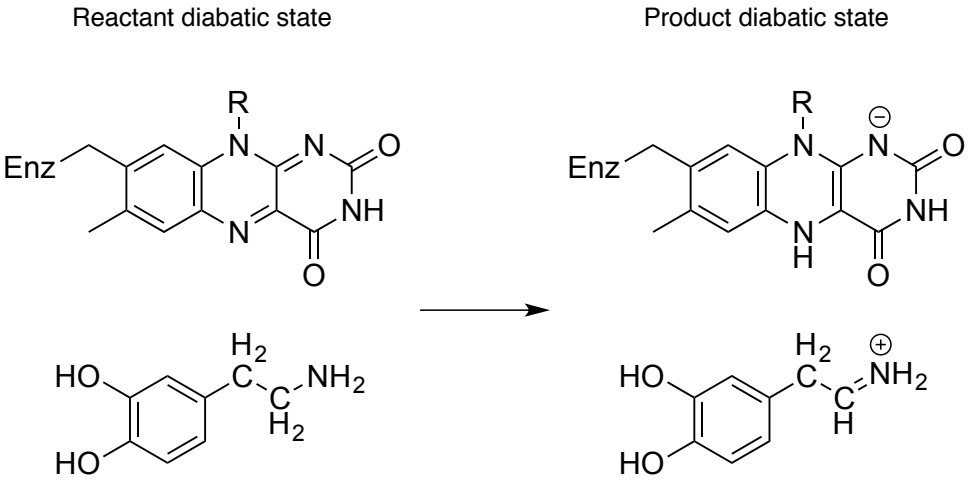

Figure 4.

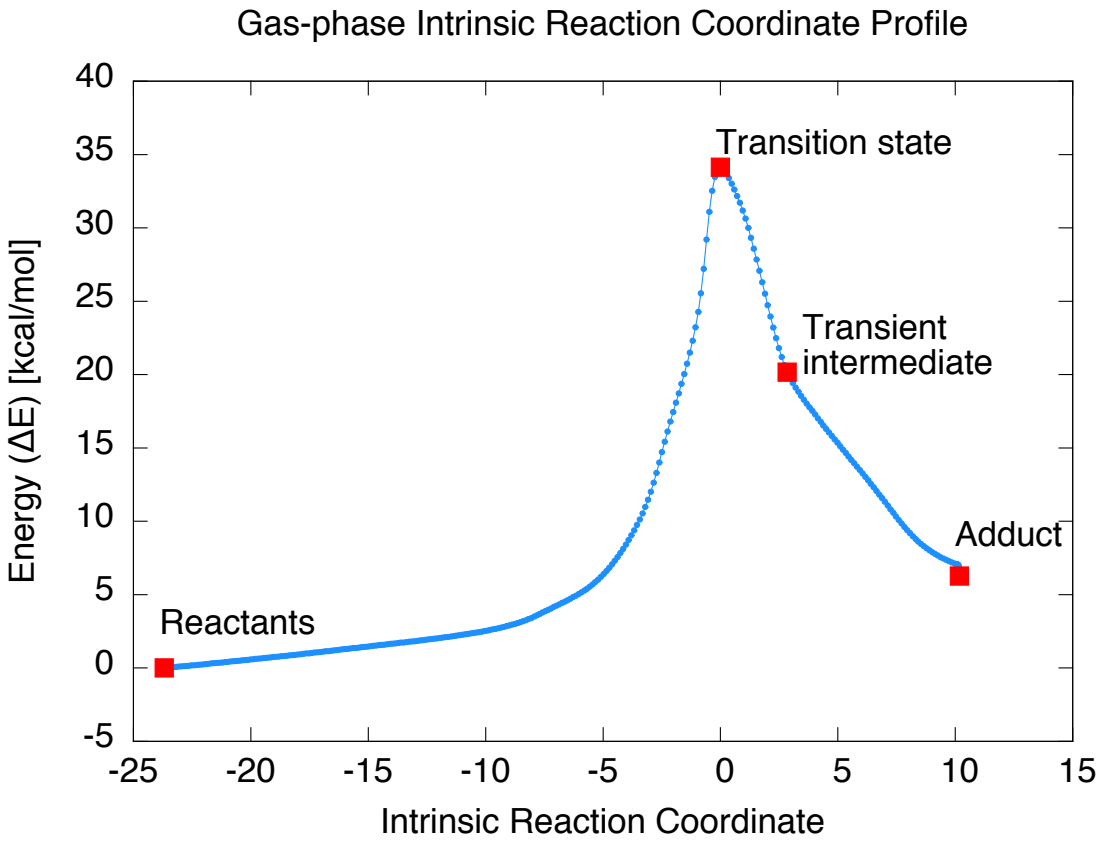
Gas-phase Intrinsic Reaction Coordinate Profile
Energy (ΔE) [kcal/mol]
Intrinsic Reaction Coordinate
Transition state
Transient intermediate
Adduct
Reactants
40
35
30
25
20
15
10
5
0
-5
-25
-20
-15
-10
-5
0
5
10
15

Figure 5.

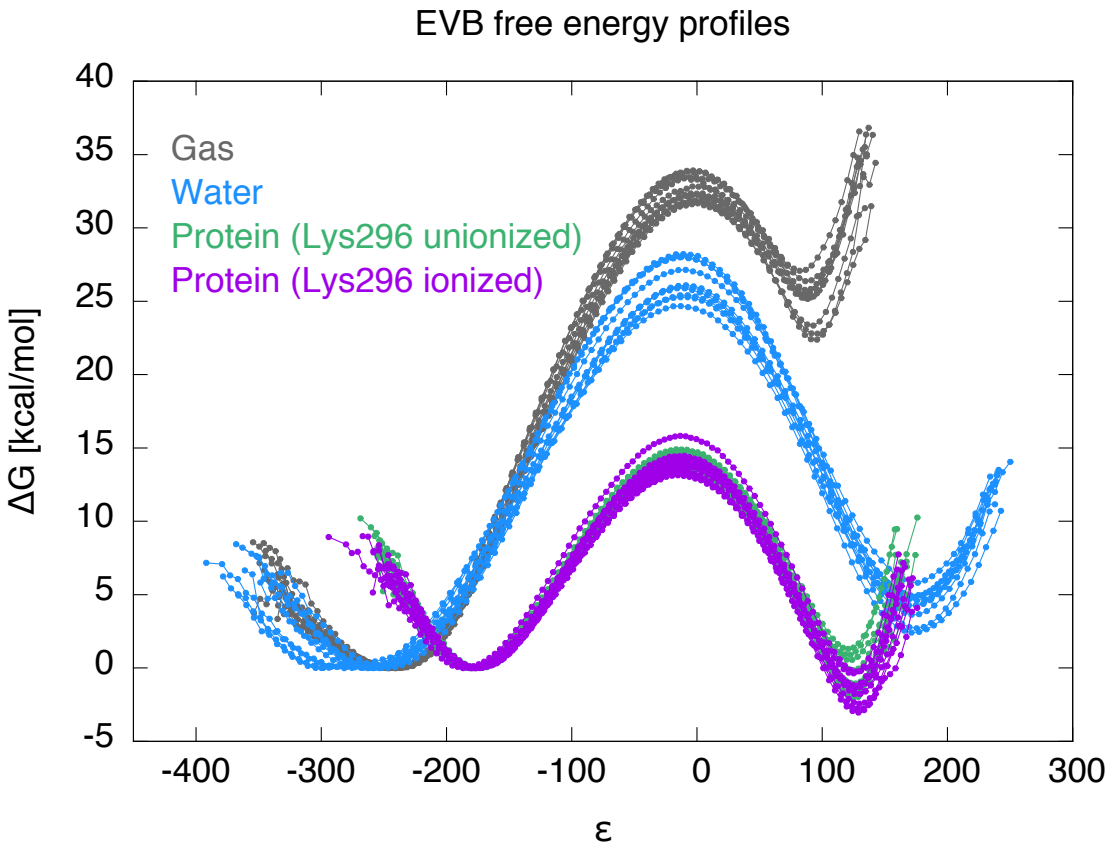
EVB free energy profiles
Gas
Water
Protein (Lys296 unionized)
Protein (Lys296 ionized)
ΔG [kcal/mol]
ε
40
35
30
25
20
15
10
5
0
-5
-400
-300
-200
-100
0
100
200
300

Figure 6.

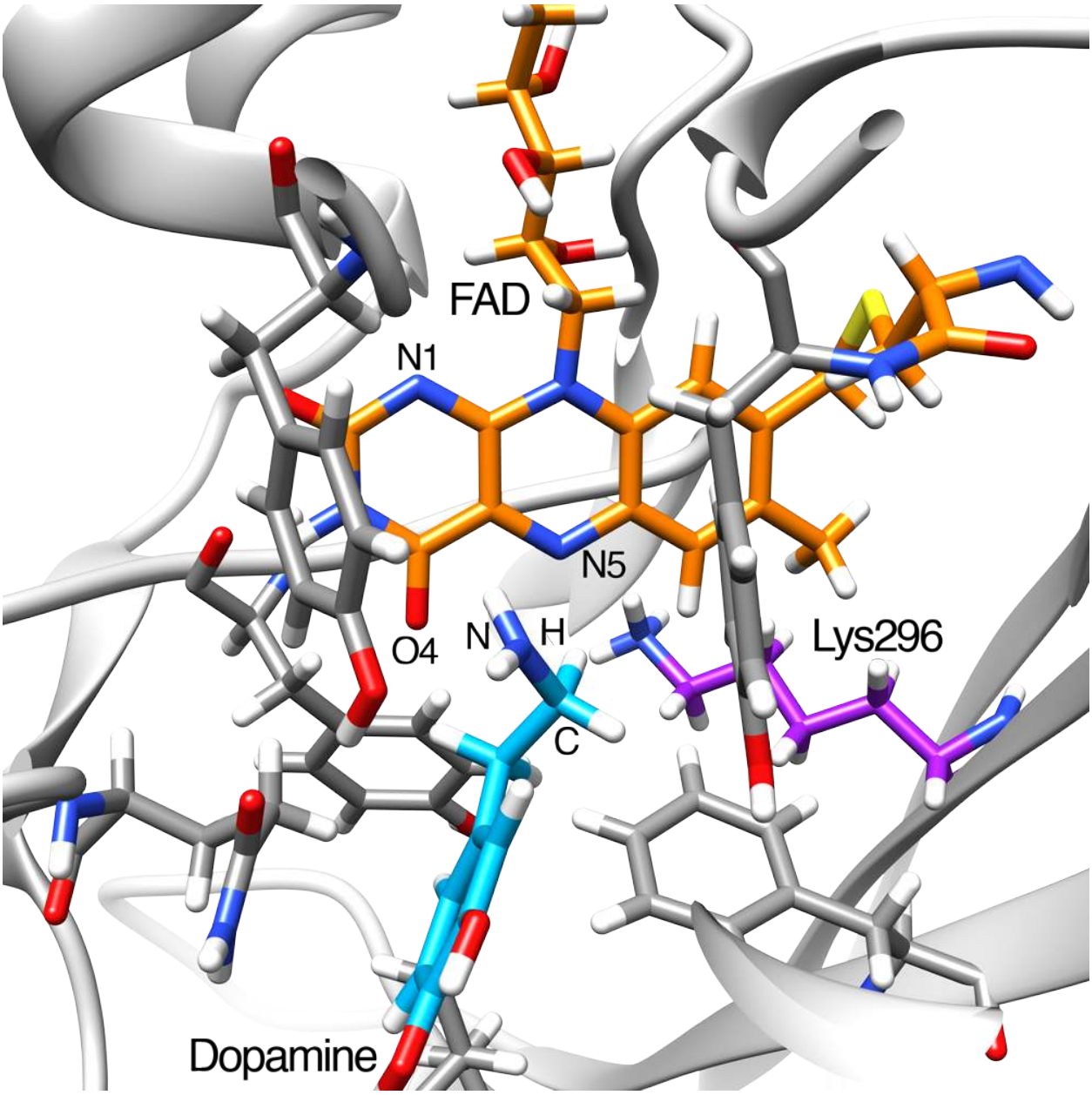

Figure 7.